Int. J. Electrochem. Sci., 17 **(2022)** Article Number: 221258, doi: 10.20964/2022.12.59

International Journal of
ELECTROCHEMICAL
SCIENCE
www.electrochemsci.org

Detection of Glioma Cells based on Electrochemical Sensor Based on an Aptamer Method Recognition

Lei Chen[1], *Shu Zhu*[2] *and Xuepeng Wang*[1,*]

[1] Department of Neurosurgery, Affiliated Hospital of Beihua University, Jilin Province, China
[2] Department of Ophthalmology, Affiliated Hospital of Beihua University, Jilin Province, China
[*]E-mail: xpwang@gmx.com

Received: 21 August 2022 / *Accepted:* 22 September 2022 / *Published:* 27 December 2022

The detection of glioma cells (GMC) could be used to evaluate the effectiveness of treatment. Based on the advantages of easy synthesis and modification of aptamers and the advantages of high sensitivity, excellent selectivity, and wide application of electrochemical methods, this work constructs an aptamer electrochemical sensor that can be used for rapid and efficient detection of GMC. We used activators for the activation of carboxyl groups after modification of 4-carboxyphenyl diazonium salt. The aptamer, which can specifically recognize GMC, is immobilized on the electrode surface by forming an amide bond between the amino and carboxyl groups on the aptamer. The conditions affecting the sensing of the aptamer sensor were investigated in detail. The current of the aptamer sensor is proportionally with the GMC concentration from 1×10^7 to 1×10^2 cells/mL. Moreover, the sensor can identify GMC with reasonable specificity.

Keywords: Aptamer. Electrochemical sensor; Cell detection; Glioma; Analysis of cancer

1. INTRODUCTION

Glioma is one of the most common central nervous system tumors and originates from various glial cells. It includes astrocytes, oligodendrocytes, and ventricular meningeal cells, characterized by rapid proliferation, poor differentiation, aggressiveness, easy surgical recurrence, and poor prognosis [1,2]. In the past, clinicians developed treatment plans based on the tumor's pathological grading and morphological characteristics and usually performed a combination of traditional surgery and radiotherapy as the primary treatment. However, the results of this type of treatment are not satisfactory [3,4]. With the continuous advancement of medical technology, immunotherapy has become the fourth treatment modality after surgery, radiotherapy, and chemotherapy. The clinical effectiveness of immunotherapy was detailed in a Meta-analysis, with a significant increase in 1-year overall survival and mean progression-free survival for patients. The effectiveness of immunotherapy is attributed to the

microenvironmental properties of gliomas. First, glioma cells express a limited number of specific antigens and thus are more likely to evade immune surveillance [5]. Second, the microenvironment contains high levels of inhibitory cytokines, such as transforming growth factor-beta and interleukin-10, which impede the activation of immune cell function [6]. Third, there are a variety of immunosuppressive cells in the microenvironment, such as cytotoxic T cells that have lost their normal function, regulatory T cells that secrete suppressive cytokines, bone marrow-derived suppressor cells, and tumor-associated macrophages. In addition to the development of effective therapies, the development of a rapid and selective glioma cell (GMC) detection technique is essential.

The GMC assay usually includes a pre-separation and enrichment phase and a post-analysis and identification phase. The amount of GMC in the blood is extremely rare, usually 1 - 100 cells/mL. The blood contains many red blood cells, white blood cells, and platelets [7,8]. The ideal GMC separation and enrichment technology should have the ability to recover GMC efficiently. The recovered GMC has high purity and is not contaminated by other cells for the following analytical assay. The obtained GMCs need to be further analyzed and characterized, and the biological information of the tumor cells is usually analyzed using immunostaining, DNA, RNA, and protein assays to assist in diagnosis and treatment [9]. Currently, nanotechnology and microfluidics are increasingly being used in cellular assays [10]. Nanostructures can enhance the interaction of cancer cells with the reaction interface. Microfluidic devices have a small footprint, low sample volume, and reagent usage, a high degree of automation, and can integrate multiple technologies [11].

In recent years, aptamer electrochemical sensors have been widely used in the pharmaceutical field. Yang et al. [12] detected and quantified trace Ag^+. Single-stranded oligonucleotide probes rich in cytidine can be immobilized on the surface or inside the composite, and the T bases on the probe strand form a stable T -Ag^+-T structure with Ag^+ when Ag^+ is present. The current signal is thus altered to enable the detection of Ag^+. Chen et al. [13] prepared signal probes by attaching magnetic mesoporous nanomaterials to Cd^{2+} and Pb^{2+} aptamers and then to aptamers of chloramphenicol and hygromycin respectively. The different electrochemical redox potentials of Cd^{2+} and Pb^{2+} can be distinguished by anodic dissolution voltammetry. This work aims to construct an aptamer electrochemical sensor for GMC detection and establish a fast, simple, and accurate method. Aptamer electrochemical sensors use nucleic acid aptamers as sensitive recognition elements for electrochemical biosensors that bind to specific targets. When the presence of the target causes a change in the structure of the aptamer, the detection of the target is achieved by the change in the signal before and after the change in the structure of the aptamer as a biosensor. The sensor is constructed by the covalent bonding method, introducing the reactive group carboxyl group, forming an amide bond with the amino group on the aptamer, and associating the aptamer to the electrode surface to achieve susceptible and selective detection of the target.

2. EXPERIMENTAL

2.1. Reagents

N-Hydroxysuccinimide (NHS), 1-(3-Dimethylaminopropyl)-3-ethylcarbodiimide hydrochloride (EDC) purchased from Beijing Soleibao Technology Co., LTD. Ethanolamine, sodium dihydrogen

phosphate, disodium hydrogen phosphate, potassium ferricyanide, and potassium ferrocyanide were purchased from Shanghai Aladdin Reagent Co., LTD. Phosphate buffered solution (PBS, 0.01 M, pH 7.4) was used as supporting electrode.

The aptamer sequence, which was from SBS Genetech Co. Ltd. and used to detect GMC, is as follow: 5′-GTA CTT CCA TTT GTG TTT GCC CGG AGC CTT AGT CTG TTC AAA AGT-3′.

2.2. GMC recovery and culture

Cell manipulation was conducted strictly following the aseptic protocol, and the ultra-clean bench was irradiated with UV light for 15 min before use. The cell freezing tubes containing GMC cell lines frozen in liquid nitrogen were quickly placed in warm water at 37°C and shaken repeatedly to make the cell solution thaw rapidly. The cytosol was transferred into a cell culture flask containing a cell culture medium (37°C) and then placed in a cell culture incubator. After 12 h, the cytosol was transferred to a 15 mL centrifuge tube and centrifuged (1500 rpm, 5 min). Discard the supernatant and add the appropriate amount of cell culture medium. The cell suspensions were transferred into cell culture flasks and then placed in a cell culture incubator for further incubation. Observe the growth status of the cells daily and change the cell culture medium every two to three days.

2.3. Validation of aptamer and GMC-specific binding

Alexa Fluor 488 was labeled on the 5′ end of the nucleic acid. The synthetic aptamer and random sequence lyophilized powder were centrifuged (10,000 rpm, 1 min). Carefully open the lid, add an appropriate amount of sterilized PBS to a final concentration of 10 mM, and store at 4°C until use. Take the culture solution containing 3×10^5 GMC, centrifuge (1000 rpm, 5 min), and discard the supernatant. Add PBS containing 1% BSA to the cell precipitate, mix well to a single cell suspension, and incubate in a water bath at 37°C for 0.5 h to close the non-specific sites on the cells. The cell suspension is then centrifuged, and the upper layer is aspirated. 1 mL of the binding buffer is added and mixed with resuspending the cells. Alexa Fluor 488-labeled nucleic acid at 15 pM is then added and mixed. The cell suspension is placed in a water bath at 37°C and protected from light for 0.5 h. The cell suspension is then centrifuged again, and the upper layer is aspirated to remove unbound aptamers. The cells were resuspended by careful puffing and mixing with binding buffer and then assayed using flow cytometry.

2.4. Construction of GmC aptamer electrochemical sensors

200 μL of 0.1 M $NaNO_2$ was added to 20 mL of a solution containing 2 mM 4-aminobenzoic acid and 0.5 mM HCl. The mixture was shaken for 5 min to produce 4-carboxyphenyl diazonium salt (4-CP). 20 μL of the reaction solution was pipetted onto the surface of the bare electrode (bare GCE), and the modified electrode was dried to obtain the 4-carboxyphenyl diazonium salt-modified GCE (4-CP/GCE). A mixture of 20 μL of 0.1 M EDC and NHS was coated on the above electrode to form A/4-CP/GCE. After 0.5 h of reaction, the electrode surface was rinsed, and 2 μ L of aptamer (2 μM) was

applied dropwise to the electrode surface to obtain AP/A/4-CP/GCE. After incubation for 12 h at 4°C, the sensor was rinsed to remove unbound aptamers, and then 20 μL of ethanolamine (1 M) was added dropwise. After 1 h, the electrode surface was rinsed and coated with 20 μL BSA (1%), left for 1 h, and rinsed. A certain amount of GMC was titrated onto the electrode surface of AP/A/4-CP/GCE and incubated for 1 h before measurement.

2.5. Electrochemical measurements

The GMC aptamer sensor construction process was characterized using cyclic voltammetry (CV) and electrochemical impedance spectroscopy (EIS). Differential pulse voltammetry (DPV) has been used for detecting GMC. A modified electrode was used as the working electrode, a saturated calomel electrode as the reference electrode, and a platinum wire electrode as the counter electrode. The current response of the modified electrode was measured in the three-electrode system in an aqueous solution containing 5.0 mM $[Fe(CN)_6]^{3-}$ and 0.1 M KCl.

3. RESULTS AND DISCUSSION

CV is a standard characterization method in electrochemistry, and the use of potassium ferricyanide as a probe allows the characterization of electrode modification.

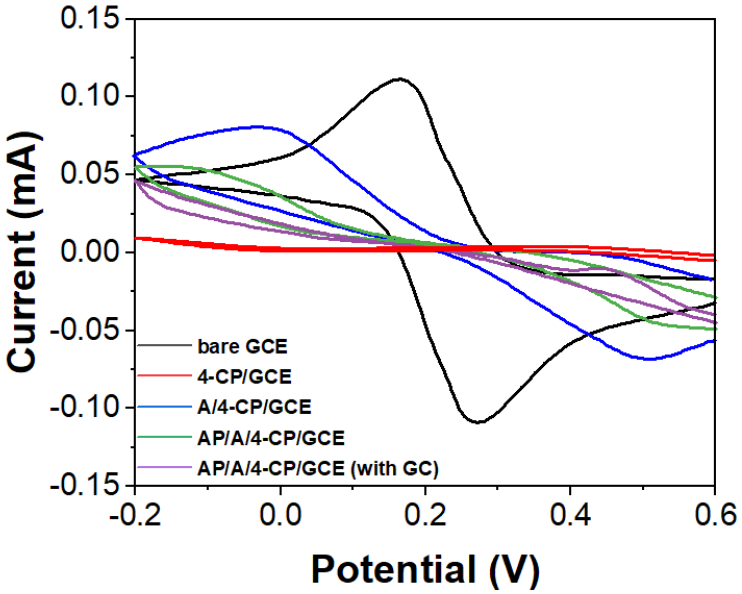

Figure 1. CVs of bare GCE, 4-CP/GCE, A/4-CP/GCE, AP/A/4-CP/GCE and AP/A/4-CP/GCE (with GMC) in 5 mM $[Fe(CN)_6]^{3-/4-}$. Scan rate: 100 mV/s.

The CV characterization of the GMC aptamer electrochemical sensor construction process is shown in Figure 1. Typical redox peaks of the potassium ferricyanide can be seen in the CV plot of the bare GCE. The CV of the bare electrode after modification of 4-CP (4-CP/GCE) shows that the anodic

and cathodic current peaks of potassium ferricyanide almost disappeared due to the organic layer formed after 4-CP modification, which hindered the electron transfer [14,15]. The negatively charged carboxyl groups can act as an electrostatic barrier. When the carboxyl group is activated, no negatively charged groups will prevent the probe from reaching the electrode, so the redox peak current appears again. The aptamer immobilization can further reduce the current [16–18]. After incubation with AP/A/4-CP/GCE in GMC (1×10^5 cells/mL) for 1 h, the binding of the analyte to the aptamer resulted in a change in the aptamer structure. This caused the CV current response values to continue to decrease.

Figure 2 exhibits the EIS characterization of different modified electrodes during the GMC aptamer electrochemical sensor construction. The EIS curve of bare GCE has the smallest resistance value. The 4-CP/GCE surface is modified with 4-CP to form a carboxyl layer, which hinders the electron transfer rate and maximizes the resistance [19,20]. The A/4-CP/GCE has reduced resistance by the absence of negatively charged groups in the activated carboxyl group. After coupling the aptamer to the electrode, the sensor resistance increase. After the aptamer binds to the target, the resistance increases due to changes in the aptamer structure [21–23]. The change of EIS during the construction of the aptamer electrochemical sensor was consistent with the response of CV. These results suggest that the GMC aptamer electrochemical sensor was successfully constructed and responded well to 1×10^5 cells/mL of GMC.

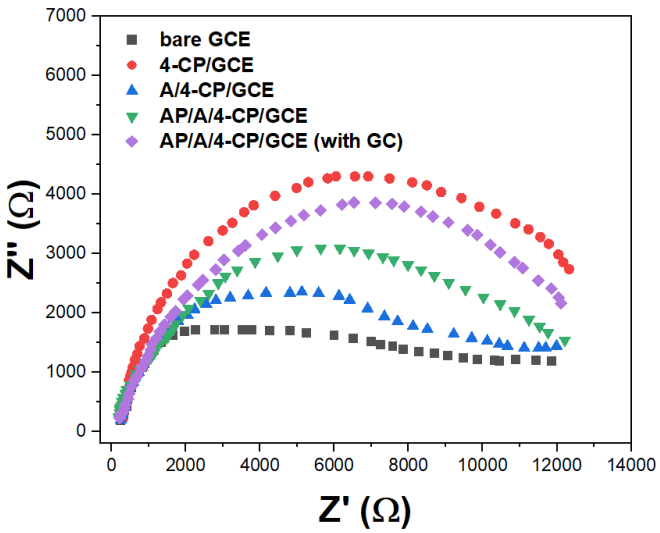

Figure 2. EIS of bare GCE, 4-CP/GCE, A/4-CP/GCE, AP/A/4-CP/GCE and AP/A/4-CP/GCE (with GMC) in 5 mM $[Fe(CN)_6]^{3-/4-}$. Frequency range: 1~10^5 Hz; amplitude: 5 mV.

SEM is a standard method used in electrochemistry to observe the surface morphology of materials. Figure 3A shows 4-CP/GCE, and it can be seen that 4-CP is well modified to the electrode. Figure 3B shows the SEM image of A/4-CP/GCE. The 4-CP structure was changed after activation.

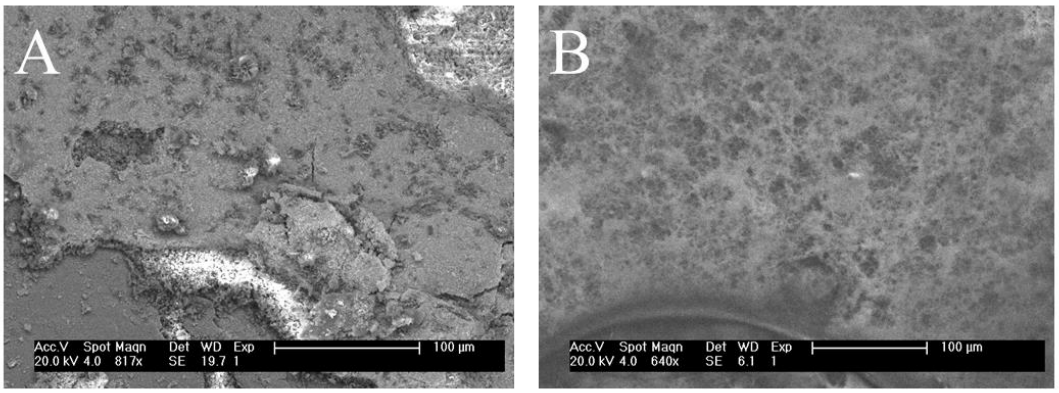

Figure 3. SEM images of (A) 4-CP/GCE and (B) act/4-CP/GCE.

The conditions affecting the sensing of the aptamer sensor, including the aptamer concentration, the binding time of the aptamer to the electrode, and the incubation time of the aptamer and GMC, were optimized in the experiment. We used different aptamer concentrations to construct electrochemical sensors with aptamer concentrations from 0.25 μM to 3 μM, and detected GMC at 1×10^5 cells/mL. As shown in Figure 4, the current response gradually decreases with increasing aptamer modification concentration in a specific range. This is because the amount of aptamer covalently bound to the electrode surface gradually increases with the aptamer modification concentration [24,25]. When the same concentration of GMC is detected, the amount of GMC binding also gradually increases, which leads to a gradual decrease in the current response. When the aptamer concentration reaches 2 μM, the GMC binding amount reaches the maximum. The current response value reaches stability and no more prolonged decreases, indicating that the modification amount of aptamer reaches the maximum [26]. Therefore, we choose this experiment's best aptamer concentration of 2 μM.

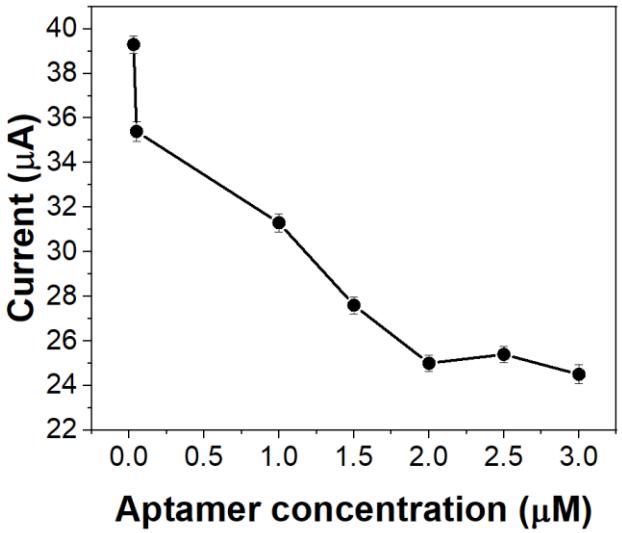

Figure 4. The current response of electrochemical sensors under different concentrations of aptamer modification toward 1×10^5 cells/mL.

The amount of aptamer covalently bound to the electrode surface varies with the binding time of the aptamer on the electrode surface, thus affecting the amount of GMC binding on the electrode surface. Therefore, the aptamer binding times of 6 h, 8 h, 10 h, 12 h, 14 h, and 16 h were selected for optimization in this experiment. The constructed aptamer electrochemical sensor was used for CV determination of GMC at 1×10^5 cells/mL, and the experimental results are shown in Figure 5. It can be seen from the figure that the current response is gradually decreasing as the aptamer binding time increases, and the amount of aptamer covalently bound to the electrode surface gradually increases [27]. When the same concentration of GMC was detected, the amount of GMC binding also increased gradually, which led to a gradual decrease in the current response. The current response stabilizes when the binding time increases to 12 h, indicating that the GMC binding amount reaches the maximum, so in this experiment, we choose the best binding time of aptamer as 12 h.

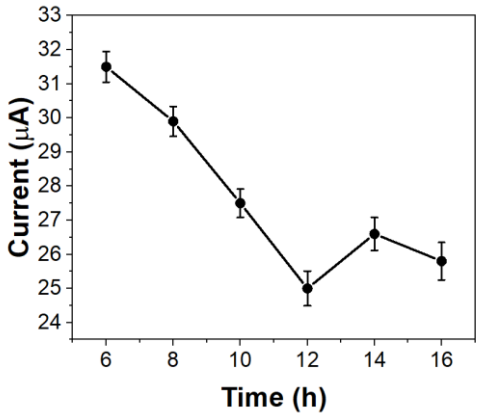

Figure 5. Current response of electrochemical sensors under different conditions of aptamer binding time toward 1×10^5 cells/mL.

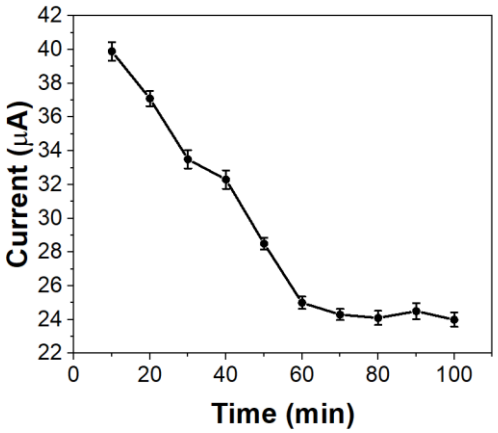

Figure 6. Current response of electrochemical sensor under different incubation times of aptamer and GMC toward 1×10^5 cells/mL.

To explore the optimal incubation time, the incubation time was optimized for the same concentration of GMC (1×10^5 cells/mL) for 15 min, 30 min, 45 min, 60 min, 75 min, 90 min, and 100

min, respectively. The results are shown in Figure 6. The current value gradually decreases with the increase of incubation before 1 h. Then, the current show no significant changes. This indicates that the binding of GMC reaches the maximum. Therefore, the optimal incubation time of 1 h was selected.

The linear detection range of the sensor is the most important index. Different concentrations of GMC (1×10^7~1×10^2 cells/mL) were detected with the constructed aptamer electrochemical sensor (Figure 7). The gradual increase of GMC concentration results in its decreasing of peak. The logarithm of GMC concentration was linearly related to the current, and the standard curve equation is y=-2.766C+3.171. These results indicate that the experimentally constructed electrochemical aptamer sensor can recognize GMC well.

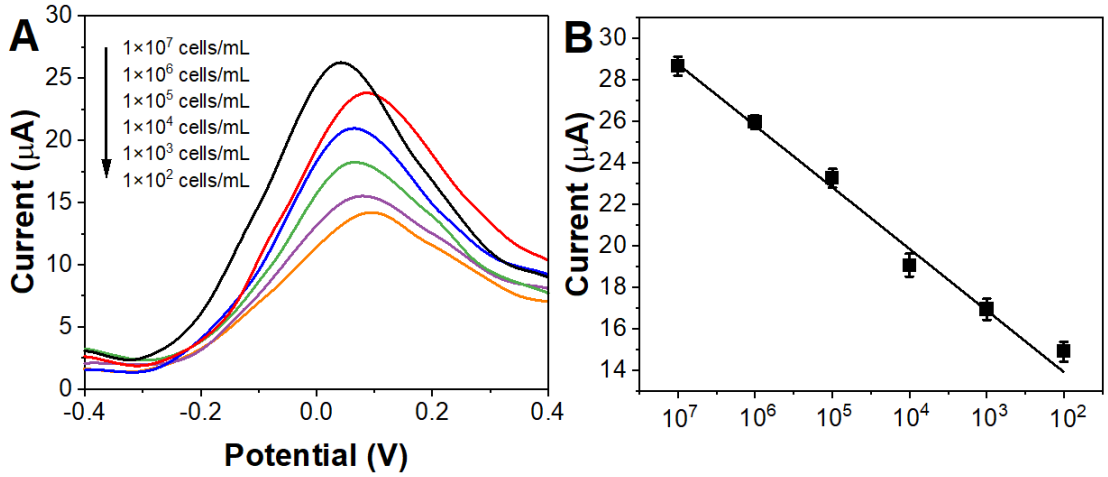

Figure 7. (A) DPV curves of AP/A/4-CP/GCE towards GMC from 1×10^2 cells/mL, 1×10^3 cells/mL, 1×10^4 cells/mL, 1×10^5 cells/mL, 1×10^6 cells/mL and 1×10^7 cells/mL. (B) Corresponding plots of GMC concentration and current responses.

The ability of the biosensor to discriminate between target cells is a crucial indicator of sensor detection performance [28]. We examined the effect of different interferents, including PBS, fetal bovine serum (FBS), bovine serum albumin (BSA), U937 cells, and Jurkat cells, on this signal biosensor. The relative current change values of PBS, FBS, and BSA were significantly lower than those of GMC ($p < 0.01$), as seen in Figure 8. The relative current change values were also very low ($p < 0.01$) when the same concentration of U937 and Jurkat cells as GMC were detected. The above results indicate that the biosensor has a strong ability to resist interference and identify GMC.

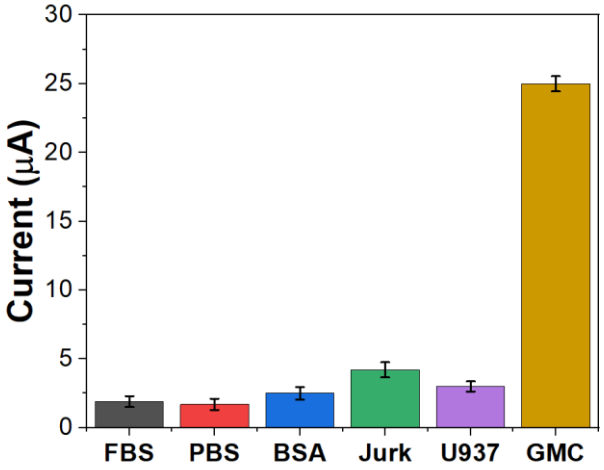

Figure 8. Current response of AP/A/4-CP/GCE towards FBS, PBS, BSA, Jurk, U937 and GmC.

4. CONCLUSION

Electrochemical biosensors are characterized by small size, short detection time, small sample size, and high sensitivity. Based on this, we established an aptamer-type electrochemical biosensing technology for the highly sensitive detection of GMC. The present work improves the stability of the sensor by anchoring the aptamer to the electrode surface by forming an amide bond between the amino group and the carboxyl group on the aptamer. After modification of the electrode surface with substances bearing carboxyl groups, we introduced EDC and NHS as activators. Activating the carboxyl group allows the aptamer to be better associated with the electrode surface for specific recognition of GMC. Under the optimal conditions, the constructed aptamer electrochemical sensor showed a linear relationship between the logarithmic value of GMC concentration and the current response in the range of 1×10^{7}~1×10^{2} cells/mL.

References

1. J. Amin, M. Sharif, M.A. Anjum, M. Raza, S.A.C. Bukhari, *Cogn. Syst. Res.*, 59 (2020) 304–311.
2. S.R. Bang-Christensen, R.S. Pedersen, M.A. Pereira, T.M. Clausen, C. Løppke, N.T. Sand, T.D. Ahrens, A.M. Jørgensen, Y.C. Lim, L. Goksøyr, *Cells*, 8 (2019) 998.
3. N. Gupta, P. Bhatele, P. Khanna, *Biomed. Signal Process. Control*, 47 (2019) 115–125.
4. Y.D. Ivanov, K.A. Malsagova, V.P. Popov, T.O. Pleshakova, A.F. Kozlov, R.A. Galiullin, I.D. Shumov, S.I. Kapustina, F.V. Tikhonenko, V.S. Ziborov, *Biosensors*, 11 (2021) 237.
5. A. Selvapandian, K. Manivannan, *Comput. Methods Programs Biomed.*, 166 (2018) 33–38.
6. C. Xu, A. Thakur, Z. Li, T. Yang, C. Zhao, Y. Li, Y. Lee, C.-M.L. Wu, *Chem. Eng. J.*, 415 (2021) 128948.
7. S. Asgarifar, A.L.G. Mestre, R.C. Félix, P.M.C. Inácio, M.L.S. Cristiano, M.C.R. Medeiros, I.M. Araújo, D.M. Power, H.L. Gomes, *Biosens. Bioelectron.*, 145 (2019) 111708.
8. B. Du, D.J. Waxman, *Cancer Lett.*, 470 (2020) 170–180.
9. Y.D. Ivanov, K.A. Malsagova, V.P. Popov, I.N. Kupriyanov, T.O. Pleshakova, R.A. Galiullin, V.S. Ziborov, A.Y. Dolgoborodov, O.F. Petrov, A.V. Miakonkikh, *Molecules*, 26 (2021) 3715.

10. J. Zhang, N. Mu, L. Liu, J. Xie, H. Feng, J. Yao, T. Chen, W. Zhu, *Biosens. Bioelectron.*, 185 (2021) 113241.
11. X. Zhu, Y. Zhu, L. Li, S. Pan, M.U. Tariq, M.A. Jan, *Sustain. Cities Soc.*, 74 (2021) 103215.
12. Y. Yang, M. Kang, S. Fang, M. Wang, L. He, X. Feng, J. Zhao, Z. Zhang, H. Zhang, *J. Alloys Compd.*, 652 (2015) 225–233.
13. M. Chen, N. Gan, Y. Zhou, T. Li, Q. Xu, Y. Cao, Y. Chen, *Sens. Actuators B Chem.*, 242 (2017) 1201–1209.
14. K. Abnous, N.M. Danesh, M.A. Nameghi, M. Ramezani, M. Alibolandi, P. Lavaee, S.M. Taghdisi, *Biosens. Bioelectron.*, 144 (2019) 111674.
15. K. Abnous, N.M. Danesh, M. Ramezani, M. Alibolandi, S.M. Taghdisi, *Biosens. Bioelectron.*, 119 (2018) 204–208.
16. S. Chung, J.-M. Moon, J. Choi, H. Hwang, Y.-B. Shim, *Biosens. Bioelectron.*, 117 (2018) 480–486.
17. M. Lang, D. Luo, G. Yang, Q. Mei, G. Feng, Y. Yang, Z. Liu, Q. Chen, L. Wu, *RSC Adv.*, 10 (2020) 36396–36403.
18. H.-K. Li, H.-L. Ye, X.-X. Zhao, X.-L. Sun, Q.-Q. Zhu, Z.-Y. Han, R. Yuan, H. He, *Chin. Chem. Lett.*, 32 (2021) 2851–2855.
19. X. Qiao, K. Li, J. Xu, N. Cheng, Q. Sheng, W. Cao, T. Yue, J. Zheng, *Biosens. Bioelectron.*, 113 (2018) 142–147.
20. S.M. Taghdisi, N.M. Danesh, M.A. Nameghi, M. Ramezani, M. Alibolandi, K. Abnous, *Biosens. Bioelectron.*, 133 (2019) 230–235.
21. J. Velayudham, V. Magudeeswaran, S.S. Paramasivam, G. Karruppaya, P. Manickam, *Mater. Lett.*, 305 (2021) 130801.
22. C. Wang, L. Liu, Q. Zhao, *ACS Sens.*, 5 (2020) 3246–3253.
23. C. Wang, Q. Zhao, *Biosens. Bioelectron.*, 167 (2020) 112478.
24. X. Wang, Y. Shan, M. Gong, X. Jin, M. Jiang, J. Xu, *Sens. Actuators B Chem.*, 281 (2019) 595–601.
25. S. Yang, Y. Teng, Q. Cao, C. Bai, Z. Fang, W. Xu, *J. Electrochem. Soc.*, 166 (2019) B23.
26. Y. Yang, X. Yang, Y. Yang, Q. Yuan, *Carbon*, 129 (2018) 380–395.
27. X. Zhang, C. Song, K. Yang, W. Hong, Y. Lu, P. Yu, L. Mao, *Anal. Chem.*, 90 (2018) 4968–4971.
28. Y. Zhou, Y. Yang, X. Deng, G. Zhang, Y. Zhang, C. Zhang, S. Shuang, Y. He, W. Sun, *Sens. Actuators B Chem.*, 276 (2018) 204–210.